International Journal of Research in Engineering and Science (IJRES)
ISSN (Online): 2320-9364, ISSN (Print): 2320-9356
www.ijres.org Volume 13 Issue 12 ǁ December 2025 ǁ PP. 154-164

3D Level Set Image Segmentation Based on FastFCM

Liang Danling[1], Liu Changjiang[1]*
[*1]*School of Mathematics and Statistics, Sichuan University of Science and Engineering, ZiGong 643000, China*
Corresponding Author: Liu Changjiang

Abstract
Aiming at the problems of initial contour sensitivity, low segmentation accuracy and poor three-dimensional segmentation efficiency in image segmentation of traditional level set methods, this paper proposes a level set image segmentation method based on Fast Fuzzy C-Means (FastFCM) initialization. Firstly, the FastFCMeans algorithm is used to coarsely segment the three-dimensional volume data to obtain the initial classification labels of different tissue regions. Secondly, the coarse segmentation results of FastFCMeans are mapped to the initial contour of the multi-phase level set function to solve the sensitive problem of the initial value of the level set. Finally, the level set energy function including bias field correction is constructed, and the high-precision three-dimensional segmentation of medical images is realized by iterative optimization. The experimental results show that the proposed method can significantly improve the segmentation accuracy and convergence speed, and can effectively deal with the gray inhomogeneity and complex tissue boundary problems in the image, which is suitable for the segmentation tasks of 3D medical image sequences such as CT/MRI.
Keywords: *FastFCM, Level Set Method, Image Segmentation, Volume Data.*

Date of Submission: 07-12-2025 Date of acceptance: 19-12-2025

I. INTRODUCTION

Image segmentation is defined as dividing the image into non-overlapping, consistent regions, which are uniform in some features such as gray value or texture. It is a key step in object recognition and classification in computer vision [1]. Now, image segmentation is widely used in automatic license plate recognition, biomedical engineering, remote sensing engineering, fire prevention and detection and other applications [2], It is the basic and key process in image processing and analysis [3, 4]. Medical image segmentation is one of the key tasks of modern medical computer-aided diagnosis. Its purpose is to accurately divide the target area [5]. However, due to the existence of anatomical geometry, partial volume effect, objects and noise, and the high time-consuming and laborious manual layer-by-layer delineation of three-dimensional medical image data, traditional manual segmentation also relies heavily on the operator’s professional knowledge, which often leads to significant variability and subjective differences. The segmentation of medical images is extremely complex [6].

At present, volume data segmentation is an important research topic in the fields of medical imaging, computer vision, computer graphics and so on. Usually, volume data comes from medical imaging (such as CT, MRI), remote sensing data (such as satellite images, lidar data) or three- dimensional models in computer graphics. Volume data segmentation can not only transform complex three-dimensional data into structured information that is easy to operate and analyze, but also improve the operability and processing efficiency of data. This process is particularly important for the medical field. It can help doctors accurately identify and locate the lesion area, assist disease diagnosis, treatment planning and surgical operation, and significantly improve the accuracy and efficiency of medical decision-making.

The difficulty of medical image segmentation is mainly due to the existence of noise, uneven intensity of pixels and other artifacts, and the image is always complex, which not only limits the process of image segmentation, but also increases the calculation time of the segmentation process. In order to deal with these problems, researchers have proposed a variety of methods or techniques. One of the most widely used methods is Fuzzy c-mean (FCM) [7, 8] algorithm [9, 10, 11, 12]. The FCM algorithm is an improvement of the ordinary C-means algorithm. The ordinary C-means algorithm is rigid for the division of data, while FCM is a flexible fuzzy division. Specifically, FCM algorithm is a partition-based clustering algorithm, which can maximize the similarity between objects divided into the same cluster, while the similarity between different clusters is the smallest. It clusters in a free way and introduces ambiguity [13] to the attribution of each image pixel. Compared with the ordinary C-means algorithm, FCM can retain more original image information.

On the other hand, the level set method based on partial differential equations (PDEs) has been proved to be very effective in biomedical image segmentation, computational fluid dynamics, trajectory planning and

other fields. Using active contour to segment images is an efficient and well-received method [14, 15]. However, the level set method is not to parameterize the active contour, but to put it into the PDE function (t, x, y). On the basis of this PDE function, we can track the zero level set (t) to determine the process of the active contour. If $(t, x, y) < 0$, it means that (x, y) is within (t), otherwise, if $(t, x, y) > 0$, it means that (x, y) is outside (t), otherwise (x, y) is at (t) [12]. The main obstacles of the level set method come from initialization constraints and time complexity.

In order to overcome these shortcomings, in this paper, we combine FCM and variational level set method to form a hybrid method. In the FCM algorithm, the image histogram is used to replace the original image data, and the computational efficiency is realized. The coarse segmentation result of the FCM algorithm is used as the initialization of the level set, which effectively solves the sensitivity problem of the level set initialization.

The organizational structure of this paper is as follows. In the second part, we introduce the related work of this paper. The third part shows the experimental results of our model. The fourth part is the conclusion.

II. THEORETICAL BACKGROUND AND RELATED WORK

Since the FCM algorithm has been well known, many researchers have added local spatial information [16, 17, 18, 19] to the original FCM algorithm to improve the performance of image segmentation [13]. For example, Ahmed et al. [20] modified the objective function of FCM to compensate for the inhomogeneity of gray (intensity), and allowed the labeling of pixels to be affected by their neighbor labels. In [21], researchers proposed a fuzzy clustering method combining spatial information to establish clustering. Adding these spatial information helps to reduce the limitations of traditional fuzzy clustering algorithms. At the same time, in order to improve the calculation speed and anti-noise efficiency of FCM, in [22, 23], the author shows how to use kernel-induced method for distance measurement, which can process medical images well.

2.1 FST FUZZY C-MEANS (FASTFCM) BASED ON GRAY HISTOGRAM)

2.1.1 FCM

Fuzzy C-means (FCM) is an unsupervised clustering algorithm, which obtains the clustering center by minimizing the objective function. The essence of the objective function is the sum of Euclidean distances from each point to each class, and the process of clustering is the process of minimizing the objective function. Nowadays, FCM algorithm has been successfully applied to many clustering problems. Given a data set $X = \{x_i, x_2, \dots, x_i, \dots x_n\} \subset R^s$, n is the number of samples, s is the dimension of the space, and its minimization objective function is as follows:

$$J_m(U, V) = \sum_{k=1}^{n} \sum_{i=1}^{c} u_{ik}^{m} \, d^2(x_k, v_i) \tag{1}$$

1

In the above expression, the FCM algorithm divides the data set into c classes, c is a positive integer greater than 1. m is a fuzzy factor, usually take 2, $d_{ij} = \|x_j - v_i\|$ represents the distance between the sample x_j and the cluster center v_i, $v_i \subset R^s$ with $1 \le i \le c$. $V = [v_1, v_2, \dots, v_n]$ is a matrix of size $c \times s$. In FCM algorithm, Euclidean distance is usually used because it is more convenient. u_{ij} represents the membership of the j sample to the i clustering center, $U = \{u_{ij}\}$ is a membership matrix of size $c \times s$, that is, the number of rows is equal to the number of clusters c, and the number of columns is equal to the number of samples n. The membership matrix represents the degree to which each sample point belongs to each class. The value of the component of the matrix U can be between 0 and 1, as long as the sum of the values of each column does not exceed 1. If all components of the U matrix are 0 or 1, the FCM algorithm will become the traditional K-means method. Therefore, the objective function of FCM has the following constraints:

$$\sum_{i=1}^{c} u_{ij} = 1, \quad 1 \le j \le n \tag{2}$$

$$u_{ij} \in [0,1], \quad 1 \le i \le c, 1 \le j \le n \tag{3}$$

$$\sum_{i=1}^{c} u_{ij} > 0, \quad 1 \le i \le c \tag{4}$$

The membership matrix U of the element u_{ik} is calculated by the following formula:

$$u_{ik} = \frac{1}{\sum_{j=1}^{c} (\frac{d_{ik}}{d_{jk}})^{\frac{2}{m-1}}} \tag{5}$$

Since each sample must belong to a cluster with a total membership degree of 1, and there is at least one data point, at most n-1 data points must belong to a cluster center. In order to minimize the objective function according to the defined constraints, the Lagrangian coefficient method can be used. At this time, the calculation formula of $V = [v_1, v_2, \dots, v_c]$ is:

$$v_i = \frac{\sum_{k=1}^{n} u_{ik}^m x_k}{\sum_{k=1}^{n} u_{ik}^m} \tag{6}$$

It can be found that u_{ik} and v_i are interrelated and contain each other. In order to determine the optimal center and relationship, the above expressions must be repeated with each other until the result value remains unchanged. Therefore, the steps of FCM algorithm are as follows:

- Select the cluster number *c* and the appropriate *m*, initialize $V^{(0)}$;
- From the iteration *t*=1 to the end of the iteration, u_{ik} is calculated according to Equation (5);
- According to the u_{ik} calculated by Equation (5), substitute it into Equation (6) to calculate v_i;
- If $\| V^{(t)} - V^{(t-1)} \| > \epsilon$, then add the iteration and return to step 2, otherwise, stop the algorithm.

Note that ϵ here is a predetermined error threshold, which is a very small constant. The above algorithm can also start from the membership matrix $U^{(0)}$.

2.1.2 FastFCM

We know that the implementation of the traditional FCM algorithm is very direct. It directly traverses all pixels of the image for calculation. When processing multi-slice images, it will lead to huge overhead in execution time and memory consumption. Although these defects can be ignored in small two-dimensional images, they are more obvious in large three-dimensional data sets, which makes it difficult to segment volume data. In order to adapt to the coarse segmentation task of 3D volume data in this paper, achieve computational efficiency, and efficiently implement these algorithms for segmenting N-dimensional grayscale images, we use the fast fuzzy C-means image segmentation (FastFCM) algorithm developed by Anton Semechko (https://github.com/AntonSemechko/Fast-Fuzzy-C-Means-Segmentation), The core is to use the histogram of image intensity to replace the original image data in the clustering process.

Let $I = [I_{\min}, I_{\max}]$ be the gray scale range of the image, then there are $l = I_{\max} - I_{\min} + 1$ in the gray scale, $H(l)$ is the number of pixels (histogram) of the gray scale I_l, that is, $\sum_{k=1}^{l} H(k) = n$, then the formula (1) can be rewritten as

$$J_m(U, V) = \sum_{k=1}^{l} \sum_{i=1}^{c} u_{ik}^m H(k) d^2(I_k, v_i) \tag{7}$$

u_{ik} represents the membership degree of gray level I_k to the i cluster, while one-dimensional gray level only requires absolute distance, so $d(I_k, v_i) = |I_k - v_i|$ represents the distance from gray level I_k to cluster center v_i.

Corresponding to, the membership degree u_{jk} and the clustering center v_i are

$$u_{jk} = \frac{1}{\sum_{i=1}^{c} (\frac{|I_k - v_j|}{|I_k - v_i|})^{\frac{2}{m-1}}} \tag{8}$$

$$v_i = \frac{\sum_{k=1}^{l} u_{jk}^m H(k) I_k}{\sum_{k=1}^{l} u_{jk}^m H(k)} \tag{9}$$

Similarly, the sum of membership of each gray level to all classes is 1, that is, $\sum_{i=1}^{c} u_{jk} = 1$.

In our experiment, we use Anton Semechko's FastFCM algorithm for coarse segmentation and initialize it by uniform sampling. In this paper, the fuzzy factors $m = 2$ and $\epsilon = 0.001$ are used. The new algorithm flow is as follows:

1. Initialization: m=2, The cluster center $V^{(0)}$ is obtained by uniform sampling

2. Iteration:

    a. Update membership degree:

$$u_{jk}=\frac{1}{\sum_{i=1}^{c}\left(\frac{|I_k-v_j|}{|I_k-v_i|}\right)^{\frac{2}{m-1}}}$$

    b. Update clustering center:

$$v_i=\frac{\sum_{k=1}^{l}u_{jk}^{m}H(k)I_k}{\sum_{k=1}^{l}u_{jk}^{m}H(k)}$$

    c. Condition of convergence: If $|V^{(t)}-V^{(t-1)}|>\epsilon$ when iterating t times, then increase the iteration and return a; otherwise, stop the algorithm.

2.2 LEVEL SET SEGMENTATION MODEL

Li [24] introduced a new region-based image segmentation method, and dealt with the intensity inhomogeneity in segmentation. Starting from the image intensity uniformity model, a natural intensity clustering method of image intensity is proposed, and the natural clustering criterion function of image intensity is defined. Now we consider a three-dimensional grayscale image $I:\Omega\rightarrow R^3$ On a given image domain Ω, for a voxel $\mathbf{x}(x,y,z)\in\Omega$ in image I, we define the local energy as

$$e_i(\mathbf{x})=\int K(\mathbf{y}-\mathbf{x})|I(\mathbf{x})-b(\mathbf{y})c_i|^2d\mathbf{y} \tag{10}$$

K is a kernel function with a standard deviation of σ. The truncated Gaussian function is defined as follows:

$$K(\mathbf{u})=\begin{cases}\frac{1}{a}e^{-|\mathbf{u}|^2/2\sigma^2}, & |\mathbf{u}|\le\rho\\ 0, & |\mathbf{u}|\ge\rho\end{cases} \tag{11}$$

Where ρ is a spherical neighborhood with radius centered on $\mathbf{y}$. a is the normalized constant such that $\int K(\mathbf{u})=1$.

The local energy $e_i(\mathbf{x})$ can be equivalently expressed as the following calculation function in the actual numerical calculation:

$$e_i(x)=I^2 1_K-2c_iI(b*K)+c_i^2(b^2*K) \tag{12}$$

where * is the convolution operation, $1_K(\mathbf{x})=\int K(\mathbf{y}-\mathbf{x})d\mathbf{y}$.

We define the following global energy as a data fitting term:

$$E=\int\sum_{i=1}^{N}\int_{\Omega_i}\left(\int K(\mathbf{y}-\mathbf{x})|I(\mathbf{x})-b(\mathbf{y})c_i|^2d\mathbf{x}\right)d\mathbf{y},\quad \mathbf{x},\mathbf{y}\in\Omega \tag{13}$$

Let ϕ be the level set function. We consider that the image domain Ω is divided into two disjoint regions Ω_1 and Ω_2. At this time, the regions Ω_1 and Ω_2 are represented by their membership functions $M_1(\phi)=H(\phi)$ and $M_2(\phi)=1-H(\phi)$, respectively. If the image domain Ω is divided into multiple disjoint regions $\Omega_1,\Omega_2,\ldots,\Omega_N$, we can use multiple level set functions $\phi_1,\phi_2,\ldots,\phi_k$ to define the membership function M_i of region $\Omega_i, i=1,\ldots,N$. there is

$$M_i(\phi_1(y),\phi_2(y),\ldots,\phi_k(y))=\begin{cases}1, & y\in\Omega_i\\ 0, & else\end{cases}$$

If $N=3$, we use two level set functions ϕ_1 and ϕ_2 to define membership functions $M_1(\phi_1,\phi_2)=H(\phi_1)H(\phi_2)$, $M_2(\phi_1,\phi_2)=H(\phi_1)(1-H(\phi_2))$ and $M_3(\phi_1,\phi_2)=1-H(\phi_1)$. If $N=4$, M_i can be defined as $M_1(\phi_1,\phi_2)=H(\phi_1)H(\phi_2)$, $M_2(\phi_1,\phi_2)=H(\phi_1)(1-H(\phi_2))$ and $M_3(\phi_1,\phi_2)=(1-H(\phi_1))H(\phi_2)$,

$M_4(\phi_1,\phi_2)=(1-H(\phi_1))(1-H(\phi_2))$, where H is the Heaviside function and $\delta_\epsilon(x)$ is the derivative of $H_\epsilon(x)$. defined as follows:

$$H_\epsilon(x) = \frac{1}{2}[1 + \frac{2}{\pi} arctan(\frac{x}{\epsilon})] \tag{14}$$

$$\delta_\epsilon(x) = H'_\epsilon(x) = \frac{1}{\pi}\frac{\epsilon}{\epsilon^2 + x^2} \tag{15}$$

Then the energy in (13) can be expressed as the following multiphase level set formula:

$$E = \int \sum_{i=1}^{N} \int_{\Omega_i} \left(\int K(y-x)|I(x) - b(y)c_i|^2 dy\right) M_i(\phi(x))dx, \quad x, y \in \Omega \tag{16}$$

Two regularization terms $\mathcal{L}(\phi)$ and $\mathcal{R}_p(\phi)$ are introduced

$$\mathcal{L}(\phi) = \int |\nabla H(\phi)|dx \tag{17}$$

$$\mathcal{R}_p(\phi) = \int p(|\nabla\phi|)dx \tag{18}$$

where $p(s)=\frac{1}{2}(s-1)^2$.

For the function $\Phi=(\phi_1,\phi_2,\dots,\phi_k)$, we define the regularization terms as $\mathcal{L}(\Phi)=\sum_{j=1}^{k}\mathcal{L}(\phi_j)$ and $\mathcal{R}_p(\Phi)=\sum_{j=1}^{k}\mathcal{R}_p(\phi_j)$. Among them, for each level set function ϕ_j, $\mathcal{L}$ and $\mathcal{R}$ are defined by (17) and (18), respectively.

In summary, the multi-phase level set formula framework is defined as

$$F = \int \sum_{i=1}^{N} \int_{\Omega_i} \left(\int K(y-x)|I(x) - b(y)c_i|^2 dy\right) M_i(\phi(x))dx$$

$$+\nu \int_\Omega \sum_{j=1}^{k} \delta_\epsilon(\phi_j(x))|\nabla\phi_j(x)|dx + \mu \int_\Omega \sum_{j=1}^{k} p(|\nabla\phi_j|)dx, \quad x, y \in \Omega \tag{19}$$

ν and μ are constants greater than 0.

The minimization of the energy F in (19) relative to the variable $\Phi = (\phi_1, \phi_2, \dots, \phi_k)$ can be achieved by solving the following gradient flow equation:

$$\begin{aligned}
\frac{\partial\phi_1}{\partial t} &= -\sum_{i=1}^{N}\frac{\partial M_i(\phi)}{\partial\phi_1}e_i + \nu\delta(\phi_1)div\left(\frac{\nabla\phi_1}{|\nabla\phi_1|}\right) \\
&\quad +\mu div\left(\left(d_p(|\nabla\phi_1|)\right)\nabla\phi_1\right) \\
&\vdots \\
\frac{\partial\phi_k}{\partial t} &= -\sum_{i=1}^{N}\frac{\partial M_i(\phi)}{\partial\phi_k}e_i + \nu\delta(\phi_k)div\left(\frac{\nabla\phi_k}{|\nabla\phi_k|}\right) \\
&\quad +\mu div\left(\left(d_p(|\nabla\phi_k|)\right)\nabla\phi_k\right)
\end{aligned} \tag{20}$$

Function $d_p(s) \triangleq \frac{p'(s)}{s}$.

Fixing ϕ and b, the optimal c such that the energy F is minimized is defined as

$$\hat{c}_i = \frac{\int (b*K)Iu_i dydx}{\int (b^2*K)u_i dydx}, \quad i=1,2,\dots,N \tag{21}$$

where $u_i(x)=M_i(\phi(x))$.

Fixing ϕ and c, and the optimal b is defined to minimize the energy F as

$$\hat{b}=\frac{(IJ^{(1)})*K}{J^{(2)}*K} \tag{22}$$

where $J^{(1)}=\sum_{i=1}^{N} c_i u_i$ and $J^{(2)}=\sum_{i=1}^{N} c_i^2 u_i$.

2.3 IMPLEMENTATION

As we know, the core of the level set function is to use the signed distance function (SDF) to describe the segmentation contour:

$$\phi(x)=\begin{cases} d(x,\partial\Omega), & x\in\Omega, \\ -d(x,\partial\Omega), & x\notin\Omega, \\ 0, & x\in\partial\Omega \end{cases} \tag{23}$$

$d(x,\partial\Omega)$ is the Euclidean distance from the pixel x to the image domain Ω boundary $\partial\Omega$.

Now we use the coarse segmentation label matrix L to initialize the level set function to avoid the subjectivity of the traditional level set to manually set the initial contour. The level set function is initialized as follows:

$$\begin{aligned} \phi_1(x,y,z)&=\begin{cases} c_0, & L(x,y,z)=1 \text{ or } 2\ (LSF1>0) \\ -c_0, & L(x,y,z)=3\ (LSF1<0) \end{cases} \\ \phi_2(x,y,z)&=\begin{cases} c_0, & L(x,y,z)=1\ (LSF2>0) \\ -c_0, & L(x,y,z)=2 \text{ or } 3\ (LSF2<0) \end{cases} \end{aligned} \tag{24}$$

where $c_0=1$ is a constant, and (x,y,z) is an arbitrary voxel of Ω in the image domain.

The main steps of the proposed model are as follows:

- Find the label L;
- According to the label results, the level set function ϕ_i is initialized using Equation (24);
- evolves the level set through formula (20), and then updates c and b according to formulas (21) and (22).

III. EXPERIMENTAL RESULTS

In this section, we will verify the ability of our method to segment 3D medical images and ICT volume data. In this paper, the clustering number $c=[2,3]$, $\mu=1$, the value range of the length term parameter is $\nu=0.001\times255^2$, and the Gaussian kernel function parameter is $\sigma=4$. Of course, we can adjust the length parameter ν according to different types of segmented images. The general rule of setting ν is: when you need to extract a smaller object, take a smaller value; if you need to segment a larger target, take a larger value. When the image is seriously uneven, a smaller σ is used.

Medical image segmentation is the core step of medical image analysis, computer-aided diagnosis (CAD) and surgical planning. Combined with the proposed segmentation method, the tissue or lesion area of interest can be accurately extracted from complex medical images. The medical images used in this paper are provided by BrainWeb: Simulated Brain Database (https://brainweb.bic.mni.mcgill.ca/brainweb/). Figure 1 shows the original image of the 22 slice of human brain MRI and the visual partition results of the two labels obtained by the FastFCM algorithm. The first column is the original image, and the second column is the label map obtained by the FastFCM algorithm. FastFCM algorithm has basically separated the target and background, which provides accurate support for the initialization of the level set. Figure 2 shows the two-dimensional segmentation results of the proposed model for human brain MRI volume data slice 5, slice 17, slice 31, slice 44 (image size is $217\times181\times50$). The segmentation details of these four slices are shown. Our model can accurately identify white matter, gray matter and cerebrospinal fluid, and the contour is smooth. It can accurately segment the target tissue and achieve superior segmentation performance.

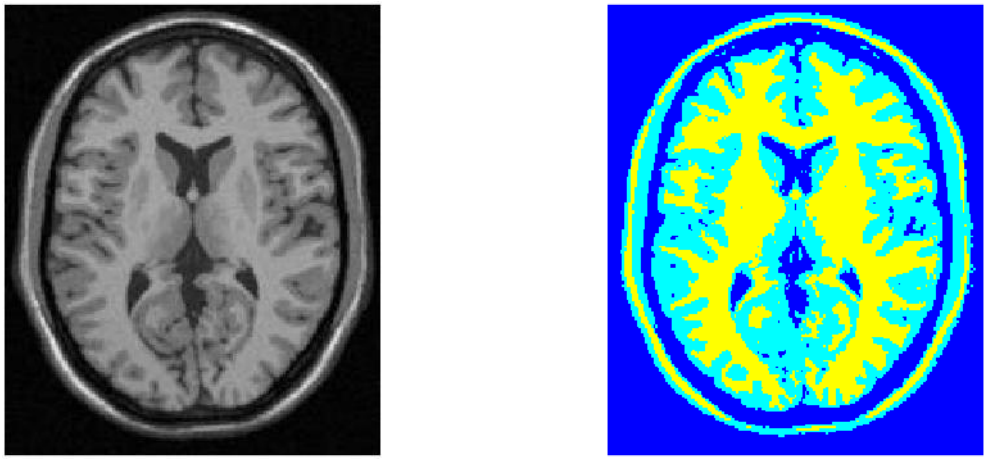

Original Image FastFCM coarse segmentation-2 class label of engine

Figure 1: FastFCM algorithm initialization comparison chart of brain.

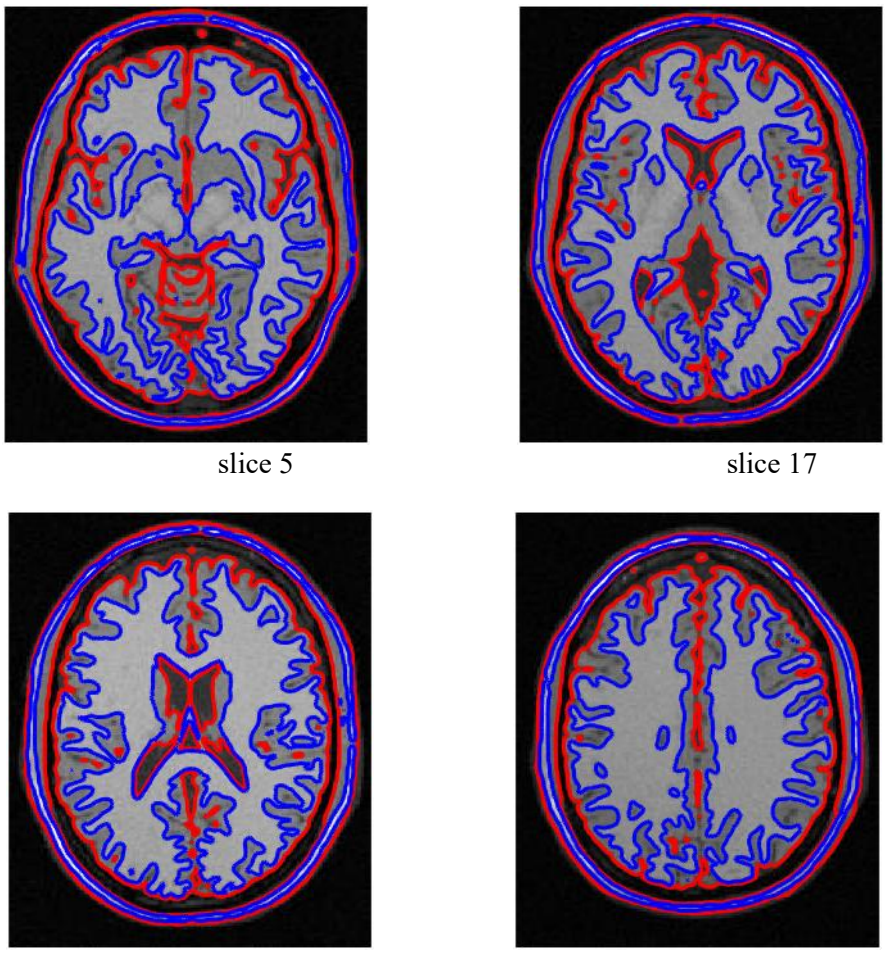

slice 5 slice 17

slice 31 slice 44

Figure 2: Segmentation results of slice 5, 17, 31, 44 of human brain CT volume data (image size $217 \times 181 \times 50$).

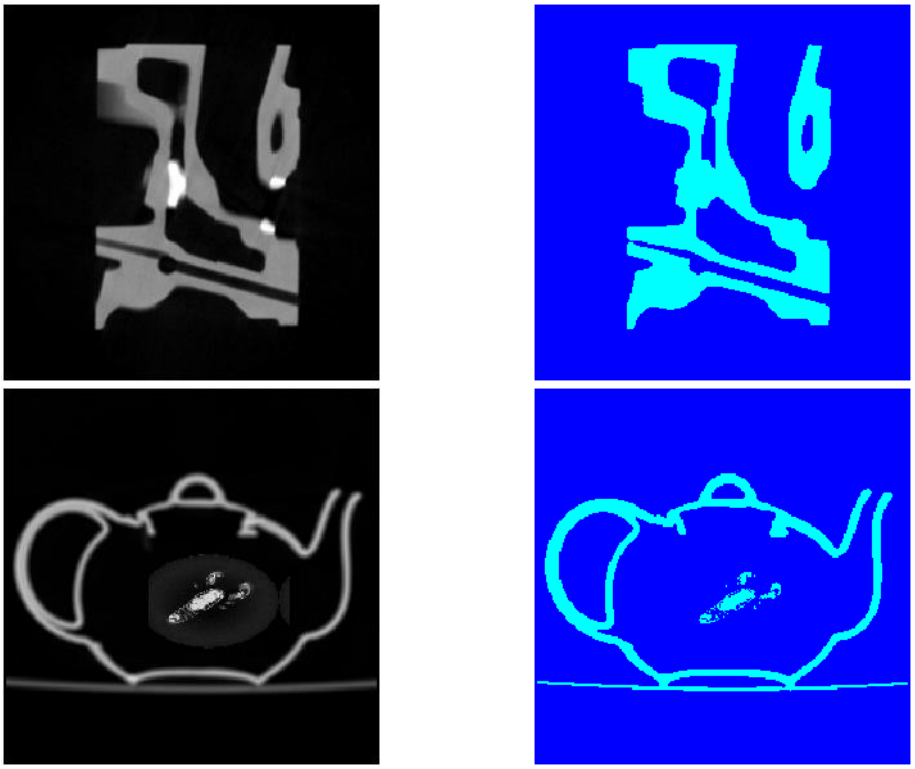

Original Image FastFCM coarse segmentation-2 class label

Figure 3: FastFCM algorithm initialization comparison chart of engine and teapot.

Tubular precision components, such as cylinders, are crucial in automobile manufacturing. Therefore, combined with the proposed segmentation method, accurate point cloud data can be obtained, making the error smaller. The car engine CT data and teapot CT data used in this paper are provided by the open scientific visualization data set (https://klacansky.com/open-scivis-datasets/category-ct.html). Figure 3 shows the original image of the 10 th slice of the engine and the teapot and the visual partition results of the two labels obtained by the FastFCM algorithm. The first column is the original image of the engine and the teapot, and the second column is the label map obtained by the FastFCM algorithm. Figure 4 shows the two-dimensional segmentation results of the proposed model for ICT volume data slice 9, slice 25, slice 38, slice 45 of engine cylinder samples (image size is $256 \times 256 \times 50$). The segmentation details of these four slices are shown. In fact, our model can accurately identify the engine cylinder, depict the edge of the object, and detect tiny holes and thin walls to achieve superior segmentation performance. Figure 6 (a) is the three-dimensional display of the engine segmentation results.

Figure 5 shows the two-dimensional segmentation results of the proposed model for the ICT volume data slice3 and slice9 of the teapot sample (the image size is $256 \times 256 \times 11$), showing the segmentation details of these two slices. According to the final evolution results, it can be seen that after the level set iteration is completed, the target contour fully fits the edge of the teapot, and the segmentation results are clear. Fig.6 (b) shows the three-dimensional display of the teapot segmentation results.

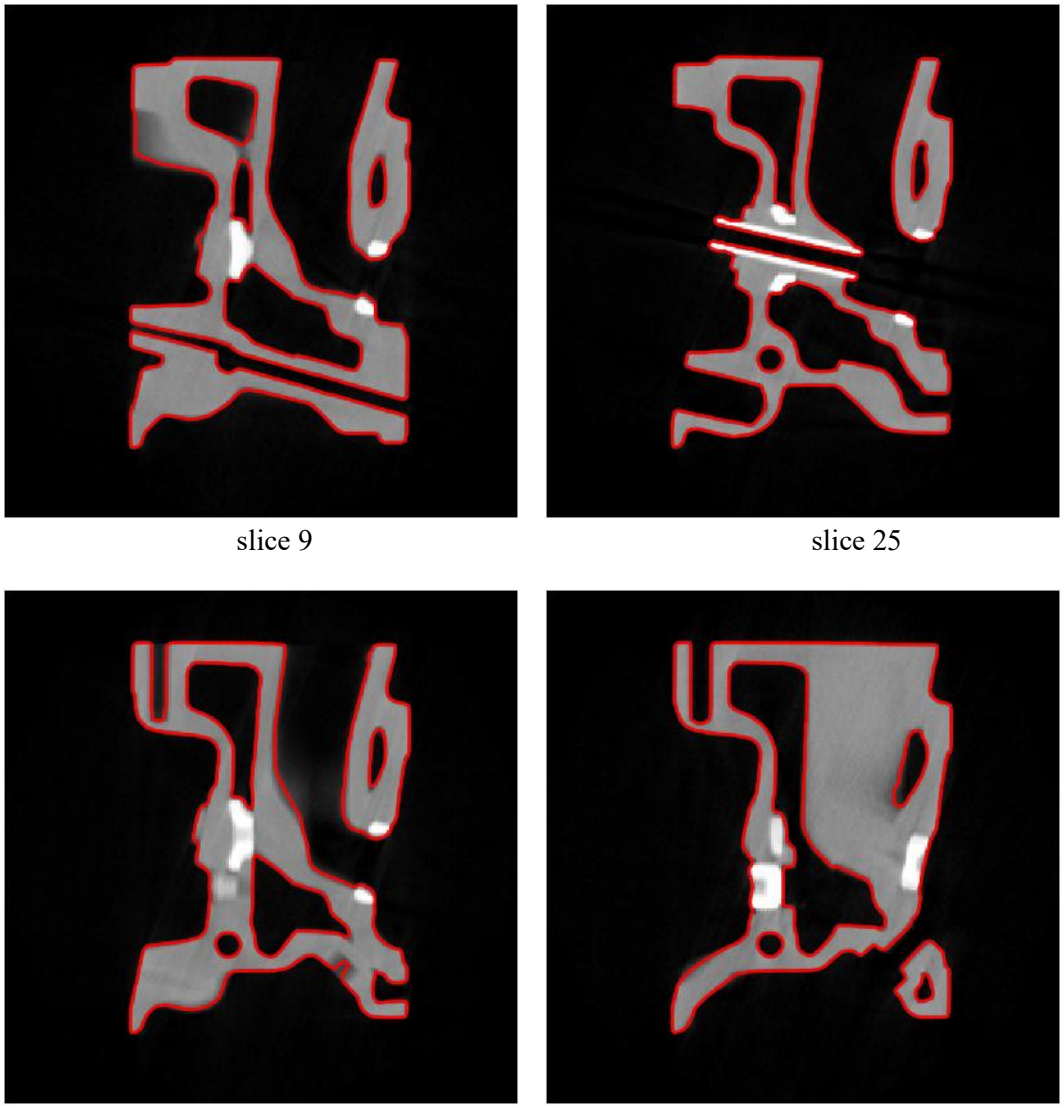

slice 9 slice 25

slice 38 slice 45

Figure 4: Segmentation results of slices 9, 25, 38,and 45 of the engine cylinder ICT volume data (image size $256 \times 256 \times 50$).

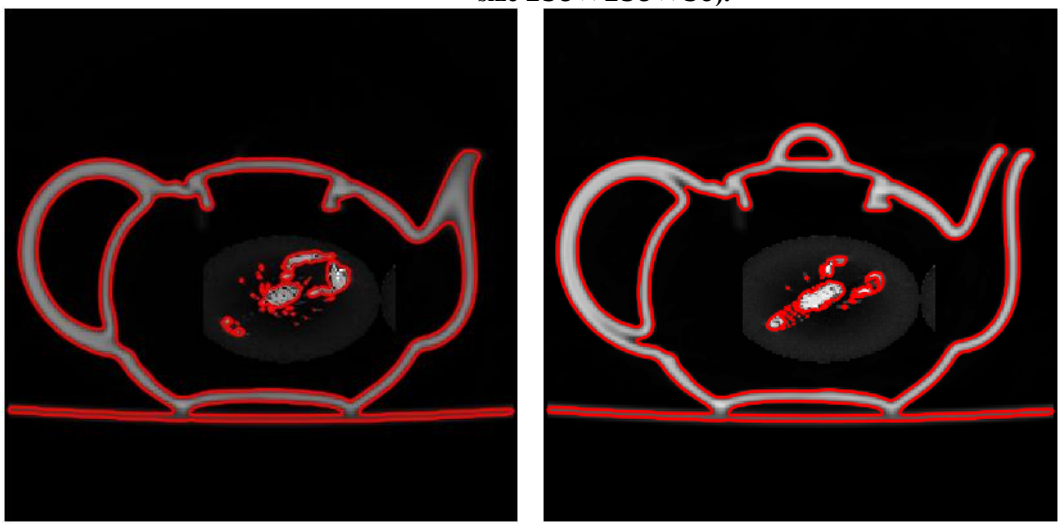

Slice 3 slice 9

Figure 5: The segmentation process of the proposed model(image size is $256 \times 256 \times 11$).

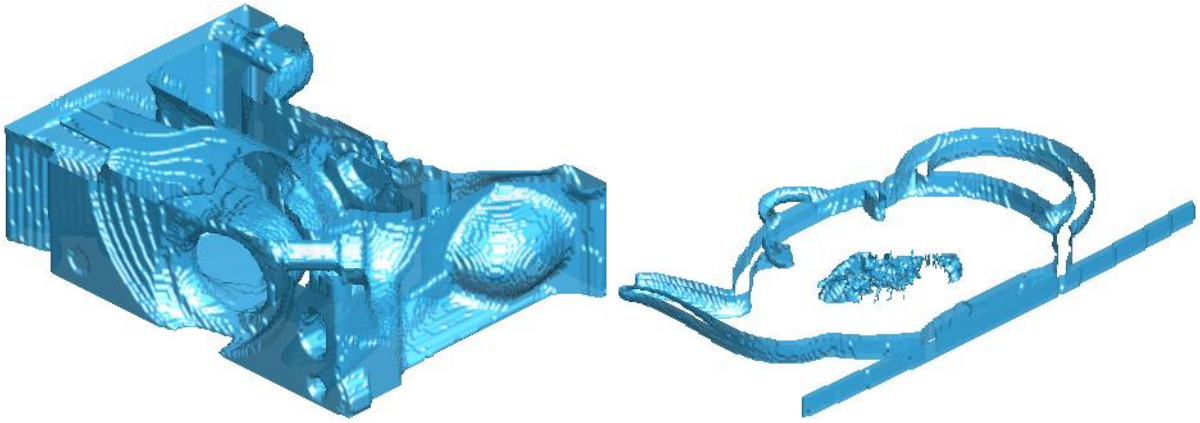

(a) (b)

Figure 6: The 3D display of the segmentation results.

IV. CONCLUSION

In this paper, a level set medical image segmentation method based on FastFCM initialization is proposed. The coarse segmentation is realized by FastFCMeans and the initial contour of the level set is generated. The fine segmentation is realized by combining the level set corrected by the bias field. The verification on BrainWeb simulated brain MRI data shows that the FastFCM algorithm can accurately complete the initial separation of the target and the background, and provide reliable initialization for the level set. Finally, the model successfully realizes the accurate segmentation of white matter, gray matter and cerebrospinal fluid. The segmentation contour of the two-dimensional slice is smooth, and the segmentation accuracy of the three-dimensional volume data is excellent. On the ICT volume data of automobile engine and teapot provided by the open scientific visualization dataset, this method shows a strong industrial detection adaptation ability, which can accurately identify the cylinder structure, depict the edge of the object, and effectively detect small holes and thin-walled features. The proposed method has both the efficiency of unsupervised initialization and the accuracy of level set segmentation. It is superior to the traditional methods in segmentation accuracy, efficiency and robustness. It can effectively deal with the problems of initial contour sensitivity, uneven gray scale and insufficient boundary extraction accuracy in the segmentation of 3D medical images and ICT volume data. Computer-aided diagnosis, surgical planning and industrial quality inspection provide reliable technical support, which has important practical application value and promotion prospects. In the future, the computational efficiency of the algorithm will be further optimized, and the GPU acceleration scheme will be explored to improve the processing efficiency of large-scale volume data, and it will be extended to medical image segmentation scenarios with multiple organs and multiple lesions.

REFERENCES

[1]. Lei, T., Jia, X., Zhang, Y., Liu, S., Meng, H., & Nandi, A. K. (2018). Superpixel-based fast fuzzy C-means clustering for color image segmentation. IEEE Transactions on Fuzzy Systems, 27(9), 1753-1766.

[2]. Cheng, Y., & Li, B. (2021, April). Image segmentation technology and its application in digital image processing. In 2021 IEEE Asia-Pacific Conference on Image Processing, Electronics and Computers (IPEC) (pp. 1174-1177). IEEE.

[3]. Radovic, D., Maksimovic, V., & Jaksic, B. (2025, March). Comparative analysis of standard image segmentation methods. In 2025 24th International Symposium INFOTEH-JAHORINA (INFOTEH) (pp. 1-5). IEEE.

[4]. Zhou C. (2024). Enhanced Sand Cat Swarm Optimization for Otsu Image Segmentation. Journal of Image and Signal Processing(4).

[5]. Song, F., Tian, Y., Gao, X., Yang, S., & Zheng, M. (2021, December). Research on medical image segmentation method. In 2021 3rd International Conference on Machine Learning, Big Data and Business Intelligence (MLBDBI) (pp. 577-580). IEEE.

[6]. Duth, P. S., Saikrishnan, V. P., & Vipuldas, V. P. (2017, April). Variational level set and level set method for mri brain image segmentation: A review. In 2017 International Conference on Communication and Signal Processing (ICCSP) (pp. 1555-1558). IEEE.

[7]. Bezdek, J. C. (2013). Pattern recognition with fuzzy objective function algorithms. Springer Science & Business Media.

[8]. Monalisa, A., Swathi, D., Karuna, Y., & Saladi, S. (2018, April). Robust intuitionistic fuzzy c-means clustering algorithm for brain image segmentation. In 2018 International Conference on Communication and Signal Processing (ICCSP) (pp. 0781-0785). IEEE.

[9]. Yamany, S. M., Farag, A. A., & Hsu, S. Y. (1999). A fuzzy hyperspectral classifier for automatic target recognition (ATR) systems. Pattern Recognition Letters, 20(11-13), 1431-1438.

[10]. Yang, M. S., Hu, Y. J., Lin, K. C. R., & Lin, C. C. L. (2002). Segmentation techniques for tissue differentiation in MRI of ophthalmology using fuzzy clustering algorithms. Magnetic Resonance Imaging, 20(2), 173-179.

[11]. Karmakar, G. C., & Dooley, L. S. (2002). A generic fuzzy rule based image segmentation algorithm. pattern recognition letters, 23(10), 1215-1227.

[12]. Mishra, A., Gupta, P., & Tewari, P. (2023, May). Biomedical image segmentation using integrated FCM clustering modified with regularized level set method. In 2023 International Conference on Disruptive Technologies (ICDT) (pp. 344-348). IEEE.

[13]. Cai, W., Chen, S., & Zhang, D. (2007). Fast and robust fuzzy c-means clustering algorithms incorporating local information for image segmentation. Pattern recognition, 40(3), 825-838.

[14]. Wu, B., Xu, S., Feng, Y., & Zhang, S. (2018, July). A new region-based active contours combined with the GAC model. In 2018 37th Chinese Control Conference (CCC) (pp. 9590-9594). IEEE.
[15]. Shervani-Tabar, N., & Vasilyev, O. V. (2018). Stabilized conservative level set method. Journal of Computational Physics, 375, 1033-1044.
[16]. Liew, A. W. C., Leung, S. H., & Lau, W. H. (2000). Fuzzy image clustering incorporating spatial continuity. IEE Proceedings-Vision, Image and Signal Processing, 147(2), 185-192.
[17]. Gendy, G. (2018, December). Adaptive fuzzy C-means algorithm using the hybrid spatial information for medical image segmentation. In 2018 9th Cairo International Biomedical Engineering Conference (CIBEC) (pp. 25-28). IEEE.
[18]. Santhalakshmi, S., & Bharathi, G. (2011, April). Local and spatial information based fuzzy C-Means clustering for color image segmentation. In 2011 3rd International conference on electronics computer technology (Vol. 3, pp. 396-400). IEEE.
[19]. Chen, H. R., Wang, X. P., Wu, J. X., & Wang, H. Z. (2024). Adaptive Semi-supervised Fuzzy C-means Method with Local Spatial Information and Pre-clustering for Image Segmentation. IEEE Access.
[20]. Ahmed, M. N., Yamany, S. M., Mohamed, N., Farag, A. A., & Moriarty, T. (2002). A modified fuzzy c-means algorithm for bias field estimation and segmentation of MRI data. IEEE transactions on medical imaging, 21(3), 193-199.
[21]. Yang, Y., Wang, R., & Feng, C. (2020). Level set formulation for automatic medical image segmentation based on fuzzy clustering. Signal Processing: Image Communication, 87, 115907.
[22]. Gharnali, B., & Alipour, S. (2018). MRI image segmentation using conditional spatial FCM based on kernel-induced distance measure. Engineering, Technology & Applied Science Research, 8(3), 2985-2990.
[23]. Memon, K. H., Memon, S., Qureshi, M. A., Alvi, M. B., Kumar, D., & Shah, R. A. (2019). Kernel possibilistic fuzzy c-means clustering with local information for image segmentation. International Journal of Fuzzy Systems, 21(1), 321-332.
[24]. Li, C., Huang, R., Ding, Z., Gatenby, J. C., Metaxas, D. N., & Gore, J. C. (2011). A level set method for image segmentation in the presence of intensity inhomogeneities with application to MRI. IEEE transactions on image processing, 20(7), 2007-2016.